Microscopic structure of coexisting 0^+ states in ^{68}Ni probed via two-neutron transfer

F. Flavigny,[1,2] J. Elseviers,[2] A. N. Andreyev,[3,4] C. Bauer,[5] V. Bildstein,[6] A. Blazhev,[7] B. A. Brown,[8] H. De Witte,[2] J. Diriken,[2,9] V. N. Fedosseev,[10] S. Franchoo,[1] R. Gernhäuser,[11] M. Huyse,[2] S. Ilieva,[5] S. Klupp,[11] Th. Kröll,[5] R. Lutter,[11] B. A. Marsh,[10] D. Mücher,[6,11] K. Nowak,[11] T. Otsuka,[12,13,14,2] J. Pakarinen,[15,16,17] N. Patronis,[18] R. Raabe,[2] F. Recchia,[19] P. Reiter,[7] T. Roger,[20] S. Sambi,[2] M. Seidlitz,[7] M. D. Seliverstov,[2,10,21] B. Siebeck,[7] Y. Tsunoda,[14] P. Van Duppen,[2] M. Vermeulen,[3] M. Von Schmid,[5] D. Voulot,[10] N. Warr,[7] F. Wenander,[10] and K. Wimmer[8,*]

[1]*Institut de Physique Nucléaire, CNRS-IN2P3, Université Paris-Sud, Université Paris-Saclay, 91406 Orsay, France*
[2]*KU Leuven, Instituut voor Kern- en Stralingsfysica, 3001 Leuven, Belgium*
[3]*Department of Physics, University of York, York, YO10 5DD, United Kingdom*
[4]*Advanced Science Research Center (ASRC), Japan Atomic Energy Agency (JAEA), Tokai-mura, Naka-gun, Ibaraki 319-1195, Japan*
[5]*Institut für Kernphysik, Technische Universität Darmstadt, Germany*
[6]*Department of Physics, University of Guelph, Guelph, Ontario N1G 2W1, Canada*
[7]*IKP, University of Cologne, D-50937 Cologne, Germany*
[8]*Department of Physics and Astronomy and National Superconducting Cyclotron Laboratory, Michigan State University, East Lansing, Michigan 48824-1321, USA*
[9]*SCK•CEN, Boeretang 200, B-2400 Mol, Belgium*
[10]*AB Department, CERN 1211, Geneva 23, Switzerland*
[11]*Physik-Departement, Technische Universität München, Garching, Germany*
[12]*Department of Physics, University of Tokyo, 7-3-1 Hongo, Bunkyo, Tokyo 113-0033, Japan*
[13]*RIKEN Nishina Center, 2-1 Hirosawa, Wako, Saitama 351-0198, Japan*
[14]*Center for Nuclear Study, University of Tokyo, 7-3-1 Hongo, Bunkyo, Tokyo 113-0033, Japan*
[15]*University of Jyvaskyla, Department of Physics, P. O. Box 35, FI-40014 University of Jyvaskyla, Finland*
[16]*Helsinki Institute of Physics, P.O. Box 64, FI-00014 University of Helsinki, Finland*
[17]*ISOLDE, CERN, Geneva 23, Switzerland*
[18]*Department of Physics, University of Ioannina, GR-45110 Ioannina, Greece*
[19]*Dipartimento di Fisica Galileo Galilei, Via Marzolo 8, 35131 Padova, Italy*
[20]*Grand Accélérateur National d'Ions Lourds (GANIL), CEA/DSM-CNRS/IN2P3, B. P. 55027, F-14076 Caen Cedex 5, France*
[21]*Petersburg Nuclear Physics Institute, NRC Kurchatov Institute, 188300 Gatchina, Russia*

(Received 23 December 2015; revised manuscript received 20 September 2018; published 31 May 2019)

The structure of low-spin states originating from shape-coexisting configurations in $^{68}_{40}Ni_{28}$ was directly probed via the two-neutron transfer reaction ^{66}Ni$(t, p)^{68}$Ni in inverse kinematics using a radioactive ion beam on a radioactive target. The direct feeding to the first excited 0^+ state was measured for center-of-mass angles 4°–16° and amounts to an integral of 4.2(16)% relative to the ground state. The observed difference in feeding of the 0^+ states is explained by the transfer of neutrons, mainly in the pf shell below $N = 40$ for the ground state, and across $N = 40$ in the $g_{9/2}$ orbital for the 0^+_2, based on second-order distorted-wave Born approximation calculations combined with state-of-the-art shell-model two-nucleon amplitudes. However, the direct feeding to the 2^+_1 state [29(3)%] is incompatible with these calculations.

DOI: 10.1103/PhysRevC.99.054332

I. INTRODUCTION

As finite many-body quantum systems, atomic nuclei are unique in the way that single-particle and collective degrees of freedom span the same energy scale. The result is a subtle interplay that leads to different configurations coexisting in the spectra of nuclei. One manifestation of this phenomenon is the variety in the nature of 0^+ states in nuclei with an even number of protons and neutrons (even-even nuclei). Besides the ground state, for which the 0^+ spin parity is a direct consequence of pairing, excited 0^+ states of different character are often present in such systems at low excitation energy. In doubly-magic nuclei the energy necessary to promote (multiple) nucleon pairs through large shell gaps is compensated by the gain due to pairing correlations creating 0^+ states with a deformed character as the lowest excitation mode. This is the case of ^{16}O and ^{40}Ca [1]. In singly-closed-shell

*Present address: Department of Physics, The University of Tokyo, 7-3-1 Hongo, Bunkyo-ku, Tokyo 113-0033, Japan.

nuclei, as a consequence of the additional correlations induced by the proton-neutron interactions, deformed 0^+ states can come very close in energy to the ground state, resulting in shape coexistence phenomena like in the remarkable case of ^{186}Pb [2], or they may even become energetically favorable and become the ground state as observed in ^{32}Mg [3,4]. Spectacularly, if the configurations involved in these coexisting states are different enough, then they can even trigger shape isomerism as recently discovered in ^{66}Ni [5,6]. Since the shape-coexistence phenomenon is now identified in several known regions with closed-proton shell and midshell neutrons [1] and could induce sudden changes of low-lying states properties in unexplored regions, unraveling precisely the microscopic configurations involved in these states has become one of the main challenges of current nuclear physics studies.

In this respect, a lot of experimental and theoretical work on ^{68}Ni, with (in a first approach) its protons filling the $Z = 28$ closed shell and its neutrons the $N = 40$ harmonic oscillator shell, has suggested this nucleus as one of the key objects of study in nuclear-structure. The low-energy spectrum of ^{68}Ni contains three known 0^+ states. The second 0^+ state (0^+_2, with the ground state being 0^+_1) is also the first excited state, with a half-life $t_{1/2} = 270(5)$ ns [7] and an excitation energy remeasured at 1604 keV using complementary probes [8–10]. The third 0^+ state (0^+_3) at 2511 keV was first observed in a β-decay experiment, resulting in a tentative spin and parity assignment [11] and confirmed later [12].

At present, a number of calculations predict the existence of the observed 0^+ (and the two 2^+) states and have to a certain extent reproduced their excitation energy [13–15]. It was suggested that the nature of the 0^+_2 state consists primarily of neutron two-particle two-hole (2p-2h) excitations from the pf shell to the neutron $g_{9/2}(\nu g_{9/2})$ orbital [13]. However, state-of-the-art large-scale shell-model calculations [14,15] point to significant mixing between the natural (0p-0h) and "intruder" (2p-2h) configurations, resulting in a remaining 0p-0h configuration content of only about 50% in the ground 0^+_1 state. The 0^+_3 state, on the other hand, is a good candidate for the proton-2p-2h excitation across the $Z = 28$ shell gap; the state was predicted at 2202 keV using neighboring 1p-2h and 2p-1h states in ^{67}Co and ^{69}Cu [16,17]. The shapes of these three 0^+ states in ^{68}Ni were studied in Monte Carlo shell-model (MCSM) calculations [15], predicting a coexistence of spherical (the 0^+_1 ground state), oblate (0^+_2), and prolate (0^+_3) shapes. The possible presence of rotational bands built on top of the 0^+_2 and 0^+_3 states, suggested by calculated quadrupole moments [14,15,18], and by observed and calculated relative transition probabilities between the 2^+ and 0^+ states [8,19], support the shape-coexistence picture.

This macroscopic picture, similar to the notable case of ^{186}Pb [2], has found in ^{68}Ni a microscopic interpretation thanks to shell-model calculations, which are still out of reach for the lead region. The advances in the production of energetic radioactive ion beams makes it now possible to probe in detail this underlying microscopic structure in the nickel region with the selectivity offered by direct reactions. Here we report on the first experimental study of the low-lying states in ^{68}Ni through the two-neutron transfer reaction ^{66}Ni(t, p) ($Q = 5.118(3)$ MeV [20]) in inverse kinematics to probe 2p-2h excitations across the $N = 40$ subshell closure. The technique used is similar to the ^{30}Mg$(t, p)^{32}$Mg transfer reaction experiment [4], where neutron excitations across the $N = 20$ harmonic oscillator shell were identified.

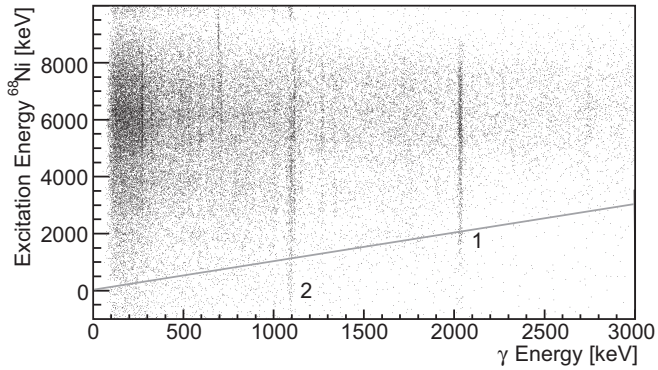

FIG. 1. Excitation energy of ^{68}Ni versus γ-ray energy in prompt coincidence with protons. The gray line is an indication for possible ground-state transitions. The numbers indicate (1) the ground-state transition from the first excited 2^+ state and (2) random events from the Doppler-broadened background line of 1039 keV arising from the β decay of ^{66}Cu.

II. EXPERIMENT

The ^{66}Ni beam (purity >99%) was produced at the ISOLDE facility in CERN [21], using the RILIS ion source [22] and was postaccelerated by REX [23,24] to 2.6 MeV/nucleon, which resulted in a center-of-mass energy of $E_{\text{c.m.}} = 7.5$ MeV. The beam with an average intensity of $2.4(3) \times 10^6$ particles per second (pps) was guided onto a tritium-loaded titanium foil [4]. The light charged recoils were detected using the T-REX silicon particle detector array [25] and the γ rays using the Miniball detection array [26]. The T-REX setup consists of a double-sided segmented annular strip detector, the CD detector [27] that covers the laboratory angles 152° to 172°, and eight position-sensitive silicon-strip detectors (the "barrel") covering the angles 27° to 78° in the forward and 103° to 152° in the backward directions. The excitation energy resolution, derived from the detected proton energy and angle, averaged to 1.3 MeV and 0.8 MeV in the forward and backward barrel detectors, respectively, and 0.22 MeV in the backward CD detector. This energy resolution originates mainly from the beam straggling in the target and variations of the target thickness over the area where the beam impinged.

III. RESULTS

Figure 1 shows the measured excitation energy of ^{68}Ni versus the detected γ energy in prompt coincidence. The gray line in the figure indicates the region for events in which a populated excited state deexcites with a γ-ray transition directly to the ground state. Only the ground-state transition from the first excited 2^+_1 state at 2033 keV was observed (marked as 1 in Fig. 1). The line marked as 2 in Fig. 1 denotes a background transition from the β decay of ^{66}Cu, the β-decay daughter of ^{66}Ni nuclei that were partially implanted in the

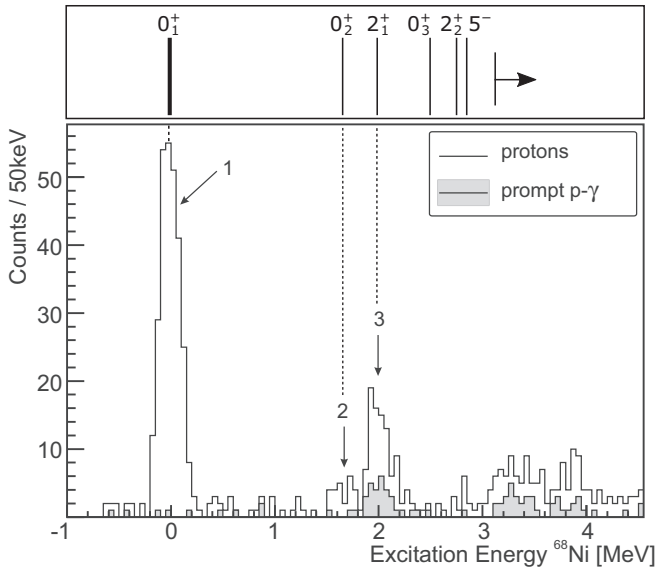

FIG. 2. Excitation energy spectrum of ^{68}Ni deduced from protons detected in the CD detector. The numbers indicate feeding to (1) the ground state, (2) the second 0^+ state, and (3) the first excited 2^+ state. The nonshaded area of the figure shows all detected protons, and the light gray area shows the protons that were detected in prompt coincidence with a γ ray. Known levels in ^{68}Ni are indicated in the panel above the figure. The pointing arrow indicates the excitation energy above which states have been omitted.

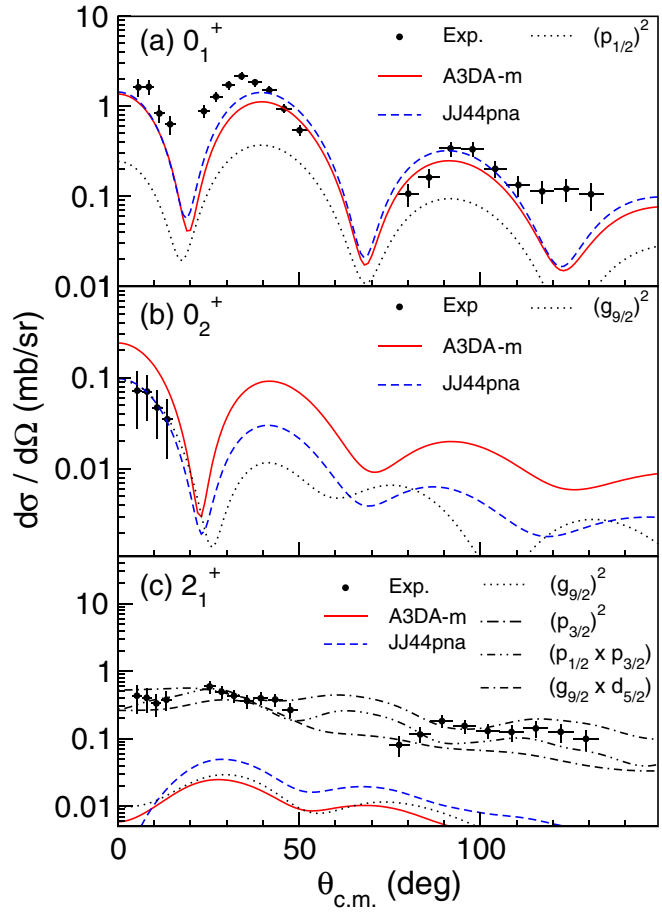

FIG. 3. Measured angular distributions together with DWBA calculations including direct and sequential transfer to the (a) ground state, (b) 0_2^+, and (c) 2_1^+ state in ^{68}Ni. Global optical model parameters are taken from Ref. [28–30]. DWBA calculations use different two-nucleon amplitudes, either from shell-model calculations with the A3DA-m interaction [15] (solid red line) or the JJ44pna interaction [31] (dashed blue line) or assuming pure two-neutron configurations (black lines). See text for details.

detection chamber. Since this β-delayed γ ray is emitted at rest, the line appears broadened and shifted due to the applied Doppler correction.

Most of the feeding in the two-neutron transfer reaction goes to high-energy states in ^{68}Ni between 5 and 9 MeV (see Fig. 1). Next to feeding to these high-energy states, strong direct feeding in the ^{66}Ni(t, p) reaction to the ground state and to the first excited 2^+ state at 2033 keV is observed. This can be seen in Fig. 2, which shows the deduced excitation energy of ^{68}Ni for protons detected in the CD detector. Figure 2 also shows a small direct-feeding component to a state at 1621(28) keV (label 2), which is identified as the 0_2^+ state observed at 1604 keV [8–10]. In contrast to the feeding to the 2_1^+ state (label 3 in Fig. 2) no prompt γ rays were detected following the population of the 0_2^+ state. Indeed, the 0_2^+ state can only decay via an $E0$ transition to the 0_1^+ ground state, which corresponds to 1.56-MeV conversion electrons with a 55% probability and to pair creation with 45% probability. The latter gives rise to 511-keV γ-ray radiation. However, this radiation was not observed because the 270(5)-ns half-life of the 0_2^+ state [7] implies that most of the ^{68}Ni recoiling ions, moving at a velocity of about 2 cm ns^{-1}, decay far upstream from the reaction chamber. The few proton-γ events that can be seen underneath this state in Fig. 2 are due to random coincidences (as visible in Fig. 1). The population of the first excited 0^+ and 2^+ states was measured to be respectively 4.2(16)% and 29.3(29)%, relative to 100% ground-state feeding, for the protons detected in the CD detector, which spans the most forward center-of-mass angles ($\theta_{c.m.} \simeq 4^\circ$ to 16°). As can be seen in Figs. 1 and 2, direct feeding to levels between 2.5 and 3.0 MeV is limited. The three states 0_3^+ at 2511 keV, 2_2^+ at 2743 keV, and 5^- at 2847 keV were treated together because they lie close in energy with respect to the proton energy resolution. An upper limit for their combined feeding of $< 2.3\%$ within a 1-σ confidence level, for the angular range of the CD detector, was determined.

IV. ANALYSIS AND DISCUSSION

Angular distributions were measured for the ground state and first excited 0^+ and 2^+ states and are shown in Fig. 3 together with two-step distorted-wave Born approximation (DWBA) calculations performed with the FRESCO code [32] including both direct and sequential transfer. Solid red lines correspond to differential cross sections calculated using two-nucleon amplitudes (TNAs) from MCSM calculations in a model space including the full pf shell plus the $0g_{9/2}$ and $1d_{5/2}$ orbitals without any truncation for both neutrons and protons (thus taking ^{40}Ca as a core) with the A3DA-m

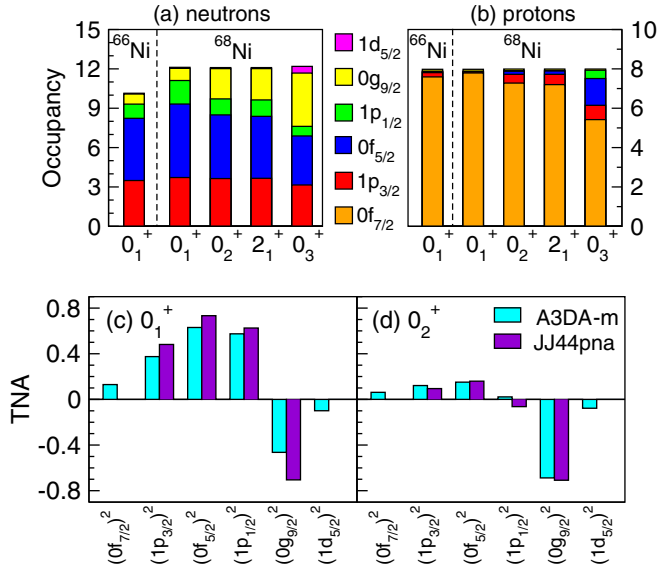

FIG. 4. Top: Average orbital occupancies of (a) neutrons and (b) protons for $0^+_{1,2,3}$ and 2^+_1 states in ^{68}Ni calculated using the A3DA-m interaction [15] (see text for details). Bottom: Two-nucleon amplitudes between the ^{66}Ni ground state and the $0^+_{1,2}$ states of ^{68}Ni [(c) and (d)] calculated using two different shell-model interactions (A3DA-m [15] and JJ44pna [31]). All of the TNA contributions in panel (c) add coherently to the two-neutron transfer cross section.

effective interaction as described in Ref. [15]. These MCSM calculations reproduce well energies of low-lying states and predict a triple-shape coexistence situation originating from strong changes of shell structure within the same nucleus driven largely by proton-neutron tensor interaction [15]. Dashed-blue lines on Fig. 3 result from the same cross-section calculations but using TNAs obtained from a shell-model calculation in the restricted neutron $0f_{5/2}$, $1p_{3/2}$, $1p_{1/2}$, $0g_{9/2}$ model space (taking ^{56}Ni as a core) with the JJ44pna effective interaction [31] and the NuShellX code [33].

In line with our main experimental observations for the $0^+_{1,2}$ states, all the calculations predict a transfer cross section to the 0^+_2 state significantly smaller compared to the ground state (21% and 9% using the A3DA-m or JJ44pna interaction, respectively). The origin of this reduced 0^+_2 population can be interpreted starting from the calculated average nucleon occupancies displayed in Figs. 4(a) and 4(b) together with the detailed components of the TNAs between the ^{66}Ni ground state and the $0^+_{1,2}$ states of ^{68}Ni [Figs. 4(c) and 4(d)]. Indeed, the average neutron occupancies displayed in Fig. 4(a) indicate that the 0^+_2 contains a strong contribution from configurations where neutrons are excited from the pf shell to the $g_{9/2}$ above the $N = 40$ gap (resulting in an average occupancy of 2.3 neutrons), whereas the 0^+_1 ground state is dominated by neutrons in the pf shell with a much lower weight of configurations with neutrons in the $g_{9/2}$ orbital (0.9 neutrons in average). With respect to the ^{66}Ni ground state, the additional neutrons in ^{68}Ni are thus mainly occupying the pf orbitals (+1.8 neutrons in average) for the ground state and the $g_{9/2}$ orbital (+1.5) for the 0^+_2 state. This structural difference between the two states, reflected in their TNAs, is enhanced in the two-neutron transfer cross sections due to the rather different matching between the pair transfer on the $g_{9/2}$ and the $p_{3/2}$, $p_{1/2}$, $f_{5/2}$ orbitals.

This is illustrated in Figs. 3(a) and 3(b), where we show with dotted lines the calculations assuming a pure $(p_{1/2})^2$ and $(g_{9/2})^2$ two-neutron transfer to the 0^+_1 and 0^+_2 (TNA = 1), respectively. Quantitatively, the pure $(g_{9/2})^2$ pair transfer above $N = 40$ is unfavored compared to the $(p_{1/2})^2$ by a factor of about 2 in the [4°–16]° angular range (12 μb/21 μb) and by a factor of about 16 in the full angular range (64 μb/1 mb). Due to this mismatch and the canceling of most of the TNA components for the 0^+_2 state apart from the $(g_{9/2})^2$ one, an overall hindrance of the cross section to the 0^+_2 is predicted and compatible with experiment.

Although this selective population mechanism seems describable schematically considering these two states as simple 0p-0h and 2p-2h configurations above the $N = 40$ gap, our study shows that the spread of TNAs over multiple components resulting from large-scale shell-model calculations is important to reach a more quantitative description of the cross section in general. This is especially clear for the ground state in Fig. 3(a) where the coherent combination of the full pfg TNA components from the shell model allows us to describe about 70% of the measured differential cross section while considering a pure $(p_{1/2})^2$ two-neutron transfer to the 0^+_1 (TNA = 1) leads only to 11%. It is true that a simpler two-state mixing approach, between the $(p_{1/2})^2$ and the $(p_{1/2})^{-2}(g_{9/2})^2$ configurations (somewhat similar to the one followed in Ref. [34]), yields two sets of mixing amplitudes, reproducing the ratio of integrated cross section between the 0^+_2 and 0^+_1 state in the covered angular range, but neither of these solutions simultaneously reproduce the absolute amplitude and shape of both angular distributions. Finally, differential cross sections calculated using the TNAs obtained with the JJ44pna interaction in a restricted model space reach a similar level of agreement with experiment than the one calculated with the A3DA-m interaction for the $0^+_{1,2}$ confirming that proton excitations above the $Z = 28$ and neutron excitation above $N = 50$ in the $\nu d_{5/2}$ orbital seem to play a reasonably minor role in the structure of these two states.

For the 2^+_1 state, different shell-model calculations with the A3DA-m [15], JJ44pna [31], and the LNPS [14] interaction link it with the 0^+_2 state and thus predict its configuration as based on neutron excitations in the $g_{9/2}$ orbital. As a result, the calculated angular distributions shown in Fig. 3(c) are similarly dominated by the $(g_{9/2})^2$ TNA component but are about an order of magnitude smaller than the experimental one. Within the current calculation framework, only a major increase of the $(p_{3/2})^2$, $(p_{1/2} \otimes p_{3/2})$, or $(g_{9/2} \otimes d_{5/2})$ TNA components could enhance the cross section enough to reproduce the magnitude of the measured cross section to the 2^+_1 state. This is illustrated in Fig. 3(c), where we plotted the calculations assuming pure configurations of this kind using dashed black lines. This result seems somewhat discrepant with the fact that measured $B(E2, 2^+_1 \rightarrow 0^+_2)$ transition strengths are well reproduced by these calculations using the same interactions [19]. On the reaction mechanism side, one could think of a coupling with another reaction channel,

for example, via the excitation of ^{66}Ni to its 2_1^+ state, but it should be very strong and mainly affect the transfer to the 2_1^+ state. To now, no indication for such a strong coupling effect exists, suggesting that the structure of this state is not entirely well described. A systematic coupled-channels study including (t, p) reaction data to neighboring isotopes [35,36], beyond the scope of this article, would be valuable to confirm it.

Finally, the measured upper limit for the population of the 0_3^+ state is consistent with the A3DA-m calculations predicting that this state would include important components of proton excitations above $Z = 28$ [see Fig. 4(b)]. The TNAs between the ^{66}Ni ground state and this 0_3^+ state in ^{68}Ni are consequently very small (all $< 5 \times 10^{-2}$), leading to a calculated cross section of 7 μb only. Intuitively, one could think that two-proton transfer is more suited to probe the structure of this state but the fact that it may involve simultaneously at least four neutrons excited above $N = 40$ (see Fig. 4(a) and Ref. [37]) could also suppress the corresponding TNAs and cross section.

V. CONCLUSIONS

The ^{66}Ni(t, p) reaction in inverse kinematics has been studied for the first time and used to assess directly the active neutrons orbitals responsible for shape coexistence in ^{68}Ni. The feeding of the 0^+ states is explained by the transfer of neutrons mainly filling the $N = 40$ subshell closure for the ground state and across $N = 40$ for the 0_2^+ state, while the low upper limit for the population of the 0_3^+ state is consistent with the prediction that this state involves also considerable proton excitations above $Z = 28$. With the recently achieved energy upgrade of HIE-ISOLDE [38], a superconducting extension of the REX postaccelerator, these studies can now be extended to higher masses to firmly characterize the microscopic origin of shape coexistence in the lead region [1,2].

ACKNOWLEDGMENTS

This work has been funded by FWO-Vlaanderen (Belgium); by BOF KU Leuven (GOA/2010/010); by the Interuniversity Attraction Poles Programme initiated by the Belgian Science Policy Office (BriX network P7/12); by the European Commission within the Seventh Framework Programme through I3-ENSAR (Contract No. RII3-CT-2010-262010); by a grant from the European Research Council (Grant No. ERC-2011-AdG-291561-HELIOS); by the German BMBF under Contracts No. 05P12WOFNF, No. 05P15WOCIA, No. 06KY9136I, No. 05P12PKFNE, No. 06DA9036I, No. 05P12RDCIA, 05P15RDCIA, and No. 05P15PKCIA + "Verbundprojekt 05P2015"; and by NSF Grant No. PHY-1811855. The MCSM calculations were performed on the K computer at RIKEN AICS (hp140210, hp150224, hp160211) and supported in part by the HPCI Strategic Program (The origin of matter and the universe) and "Priority Issue on post-K computer" (Elucidation of the Fundamental Laws and Evolution of the Universe) from MEXT and JICFuS.

[1] K. Heyde and J. L. Wood, Rev. Mod. Phys. **83**, 1467 (2011).
[2] A. N. Andreyev *et al.*, Nature **405**, 430 (2000).
[3] T. Motobayashi *et al.*, Phys. Lett. B **346**, 9 (1995).
[4] K. Wimmer *et al.*, Phys. Rev. Lett. **105**, 252501 (2010).
[5] S. Leoni *et al.*, Phys. Rev. Lett. **118**, 162502 (2017).
[6] B. Olaizola *et al.*, Phys. Rev. C **95**, 061303(R) (2017).
[7] O. Sorlin *et al.*, Phys. Rev. Lett. **88**, 092501 (2002).
[8] F. Recchia, C. J. Chiara, R. V. F. Janssens, D. Weisshaar, A. Gade, W. B. Walters, M. Albers, M. Alcorta, V. M. Bader, T. Baugher, D. Bazin, J. S. Berryman, P. F. Bertone, B. A. Brown, C. M. Campbell, M. P. Carpenter, J. Chen, H. L. Crawford, H. M. David, D. T. Doherty, C. R. Hoffman, F. G. Kondev, A. Korichi, C. Langer, N. Larson, T. Lauritsen, S. N. Liddick, E. Lunderberg, A. O. Macchiavelli, S. Noji, C. Prokop, A. M. Rogers, D. Seweryniak, S. R. Stroberg, S. Suchyta, S. Williams, K. Wimmer, and S. Zhu, Phys. Rev. C **88**, 041302(R) (2013).
[9] F. Flavigny *et al.*, Phys. Rev. C **91**, 034310 (2015).
[10] S. Suchyta, S. N. Liddick, Y. Tsunoda, T. Otsuka, M. B. Bennett, A. Chemey, M. Honma, N. Larson, C. J. Prokop, S. J. Quinn, N. Shimizu, A. Simon, A. Spyrou, V. Tripathi, Y. Utsuno, and J. M. Von Moss, Phys. Rev. C **89**, 021301(R) (2014).
[11] W. F. Mueller *et al.*, Phys. Rev. C **61**, 054308 (2000).
[12] C. J. Chiara, R. Broda, W. B. Walters, R. V. F. Janssens, M. Albers, M. Alcorta, P. F. Bertone, M. P. Carpenter, C. R. Hoffman, T. Lauritsen, A. M. Rogers, D. Seweryniak, S. Zhu, F. G. Kondev, B. Fornal, W. Krolas, J. Wrzesinski, N. Larson, S. N. Liddick, C. Prokop, S. Suchyta, H. M. David, and D. T. Doherty, Phys. Rev. C **86**, 041304(R) (2012).
[13] K. Kaneko, M. Hasegawa, T. Mizusaki, and Y. Sun, Phys. Rev. C **74**, 024321 (2006).
[14] S. M. Lenzi, F. Nowacki, A. Poves, and K. Sieja, Phys. Rev. C **82**, 054301 (2010).
[15] Y. Tsunoda, T. Otsuka, N. Shimizu, M. Honma, and Y. Utsuno, Phys. Rev. C **89**, 031301(R) (2014).
[16] D. Pauwels, O. Ivanov, N. Bree, J. Buscher, T. E. Cocolios, J. Gentens, M. Huyse, A. Korgul, Y. Kudryavtsev, R. Raabe, M. Sawicka, I. Stefanescu, J. Vande Walle, P. Vanden Bergh, P. Van Duppen, and W. B. Walters, Phys. Rev. C **78**, 041307(R) (2008).
[17] D. Pauwels, J. L. Wood, K. Heyde, M. Huyse, R. Julin, and P. Van Duppen, Phys. Rev. C **82**, 027304 (2010).
[18] A. Dijon, E. Clement, G. de France, G. de Angelis, G. Duchene, J. Dudouet, S. Franchoo, A. Gadea, A. Gottardo, T. Huyuk, B. Jacquot, A. Kusoglu, D. Lebhertz, G. Lehaut, M. Martini, D. R. Napoli, F. Nowacki, S. Peru, A. Poves, F. Recchia, N. Redon, E. Sahin, C. Schmitt, M. Sferrazza, K. Sieja, O. Stezowski, J. J. Valiente-Dobon, A. Vancraeyenest, and Y. Zheng, Phys. Rev. C **85**, 031301(R) (2012).
[19] B. P. Crider *et al.*, Phys. Lett. B **763**, 108 (2016).
[20] G. Audi, A. H. Wapstra, and C. Thibault, Nucl. Phys. A **729**, 337 (2003).
[21] R. Catherall, J. Phys. G: Nucl. Part. Phys. **44**, 094002 (2017).
[22] V. N. Fedoseyev *et al.*, Hyperfine Interact. **127**, 409 (2000).
[23] D. Habs *et al.*, Hyperfine Interact. **129**, 43 (2000).

[24] D. Voulot *et al.*, Nucl. Instr. Meth. B **266**, 4103 (2008).
[25] V. Bildstein *et al.*, Eur. Phys. J. A **48**, 85 (2012).
[26] N. Warr *et al.*, Eur. Phys. J. A **49**, 40 (2013).
[27] A. Ostrowski *et al.*, Nucl. Instrum. Methods A **480**, 448 (2002).
[28] C. M. Perey and F. G. Perey, At. Data Nucl. Data Tables **17**, 1 (1976).
[29] A. J. Koning and J. P. Delaroche, Nucl. Phys. A **713**, 231 (2003).
[30] Y. Han, Y. Shi, and Q. Shen, Phys. Rev. C **74**, 044615 (2006).
[31] A. F. Lisetskiy, B. A. Brown, M. Horoi, and H. Grawe, Phys. Rev. C **70**, 044314 (2004).
[32] I. Thompson, Comput. Phys. Rep. **7**, 167 (1988).
[33] B. A. Brown and W. D. M. Rae, Nucl. Data Sheets **120**, 115 (2014).
[34] J. A. Lay, L. Fortunato, and A. Vitturi, Phys. Rev. C **89**, 034618 (2014).
[35] W. P. Alford, R. N. Boyd, E. Sugarbaker, D. L. Hanson, and E. R. Flynn, Phys. Rev. C **21**, 1203 (1980).
[36] W. Darcey, R. Chapman, and S. Hinds, Nucl. Phys. A **170**, 253 (1971).
[37] T. Otsuka and Y. Tsunoda, J. Phys. G **170**, 024009 (2016).
[38] M. J. G. Borge, Nucl. Instrum. Methods B **376**, 408 (2016).